

Letters

ZVS of Power MOSFETs Revisited

Matthias Kasper, *Student Member, IEEE*, Ralph M. Burkart, *Student Member, IEEE*, Gerald Deboy, *Member, IEEE*, and Johann W. Kolar, *Fellow, IEEE*

Abstract—Aiming for converters with high efficiency and high power density demands converter topologies with zero-voltage switching (ZVS) capabilities. This letter shows that in order to determine whether ZVS is provided at a given operating point, the stored charge within the MOSFETs has to be considered and the condition $LI^2 \geq 2Q_{\text{oss}}V_{\text{DC}}$ has to be fulfilled. In the case of incomplete soft switching, nonzero losses occur which are analytically derived and experimentally verified in this letter. Furthermore, the issue of nonideal soft-switching behavior of Si superjunction MOSFETs is addressed.

Index Terms—Power MOSFET, zero-voltage switching (ZVS).

I. INTRODUCTION

WITH the emergence of wide bandgap semiconductors such as SiC JFETs and MOSFETs and GaN HEMTs, power electronic converters have seen a significant performance increase due to the improved figure-of-merit ($\text{FOM} = 1/\sqrt{R_{\text{DS, on}}C_{\text{oss}}}$ [1]) of these devices compared to traditional Si semiconductors. The improved switching performance allows us to operate systems at higher switching frequencies and, thus, to reduce the size of passive components. At high frequencies, however, the switching losses become a limiting factor again even for wide bandgap semiconductors. Thus, topologies providing soft switching are preferred such as, e.g., phase-shift full-bridge (PSFB), dual active bridge (DAB) or cascaded buck–boost converters [2] for dc–dc conversion, and triangular current mode (TCM) boost converter [3] for power factor corrected (PFC) ac–dc conversion, as shown in Fig. 1. For a design and optimization of a converter system with zero-voltage switching (ZVS), it is crucial to identify the conditions under which soft switching can be achieved. A basic requirement for ZVS is a semiconductor half-bridge with an inductive element connected to the midpoint, which is also common to the topologies of Fig. 1. In order to calculate the required energy stored in the inductive component at the beginning of a switching transition for achieving soft switching, a practical approach such as presented in [4] can be used.

Manuscript received March 29, 2016; revised May 06, 2016; accepted May 28, 2016. Date of publication June 01, 2016; date of current version July 08, 2016.

M. Kasper, R. M. Burkart and J. W. Kolar are with the Power Electronic Systems Laboratory, Department of Electrical Engineering, ETH Zurich, Zurich 8092 8092, Switzerland (e-mail: kasper@lem.ee.ethz.ch; burkart@lem.ee.ethz.ch; kolar@lem.ee.ethz.ch).

G. Deboy is with the Infineon Technologies AG, Villach 9500, Austria (e-mail: gerald.deboy@infineon.com).

Color versions of one or more of the figures in this paper are available online at <http://ieeexplore.ieee.org>.

Digital Object Identifier 10.1109/TPEL.2016.2574998

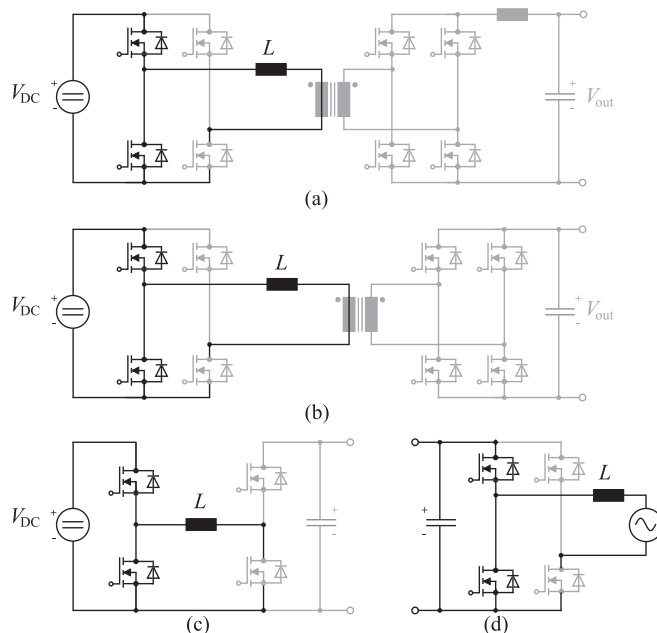


Fig. 1. Popular ZVS converter topologies: (a) PSFB converter, (b) DAB converter, (c) cascaded buck–boost converter with constant switching frequency ZVS modulation [2], and (d) TCM PFC rectifier. The basic structure of all soft-switching topologies consisting of a MOSFET bridge leg and an output inductance L is highlighted.

This letter, however, introduces an analytical approach to specify the conditions for ZVS, which only relies on data sheet values of the semiconductors. At first, the nonlinear behavior of the parasitic MOSFET capacitances is described in Section II. Section III analyzes the conditions to achieve ideal soft switching. In Section IV, analytical formulas are presented that allow to calculate the losses associated with incomplete soft switching, i.e., turn-on of switches at nonzero voltage. The derived equations are validated with measurements on different hardware setups with different types of semiconductors in Section V. Finally, Section VI summarizes the key results of this letter.

II. NONLINEAR PARASITIC MOSFET CAPACITANCES

It is widely known that the parasitic output capacitance C_{oss} of MOSFETs exhibits a nonlinear dependence on the applied drain–source voltage V_{DS} , which is shown in Fig. 2(a) for a low-voltage Si MOSFET (BS046N100NS3/Infineon). Due to this nonlinearity, the charge stored in parasitic capacitances is also a function of the applied voltage, as shown in Fig. 2(b) for the charge Q_{oss} stored in C_{oss} . In order to facilitate the modeling of

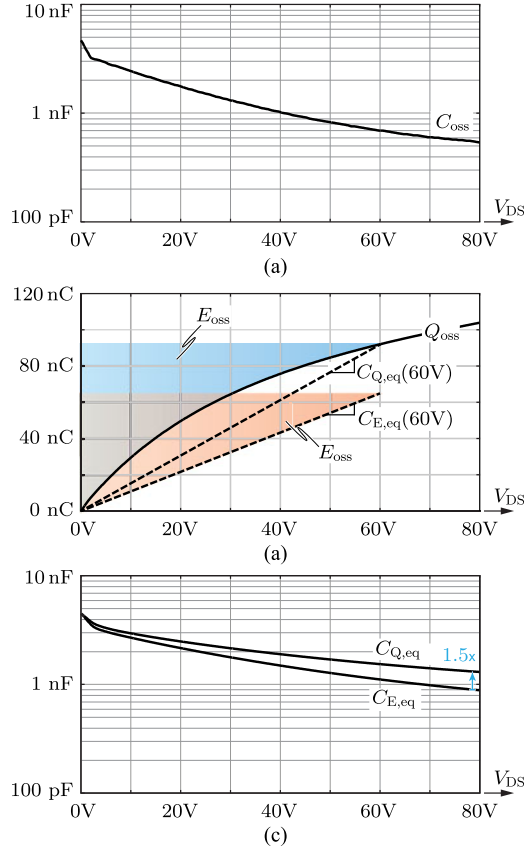


Fig. 2. Nonlinear behavior of parasitic MOSFET capacitances: (a) parasitic capacitance C_{oss} in function of the applied drain–source voltage V_{DS} as provided by the datasheet (BS046N100NS3/Infineon); (b) charge Q_{oss} stored in C_{oss} as a function of V_{DS} , charge-equivalent capacitance $C_{Q,eq}$, and energy-equivalent capacitance $C_{E,eq}$ for a drain–source voltage of $V_{DS} = 60$ V; (c) calculated values of $C_{Q,eq}$ and $C_{E,eq}$ in dependence of the drain–source voltage.

MOSFETs, a linear charge-equivalent capacitance $C_{Q,eq}$ can be introduced which exhibits the same amount of stored charge as the nonlinear capacitance at a given drain–source voltage V_{DS} [5], i.e.,

$$C_{Q,eq}(V_{DS}) = \frac{Q_{oss}(V_{DS})}{V_{DS}} = \frac{\int_0^{V_{DS}} C_{oss}(v) dv}{V_{DS}}. \quad (1)$$

In a similar way, the energy E_{oss} stored in the nonlinear capacitance C_{oss} can be determined. In Fig. 2(b), the blue shaded area enclosed between the graph of the charge Q_{oss} and the y-axis equals the energy which is stored in C_{oss} at a given voltage V_{DS} . Thus, a linear energy-equivalent capacitance $C_{E,eq}$ that stores the same amount of energy as C_{oss} at a selected voltage V_{DS} needs to have the same enclosed area, i.e.,

$$C_{E,eq}(V_{DS}) = \frac{2 \cdot E_{oss}(V_{DS})}{V_{DS}^2} = \frac{2 \cdot \int_0^{V_{DS}} v \cdot C_{oss}(v) dv}{V_{DS}^2}. \quad (2)$$

As a result, the energy-equivalent capacitance $C_{E,eq}$ and the charge-equivalent capacitance $C_{Q,eq}$ can be calculated for every drain–source voltage V_{DS} [cf., Fig. 2(c)]. It can be seen that the values of these capacitances differ by a factor of up to $C_{Q,eq}(V_{DS,max})/C_{E,eq}(V_{DS,max}) = 1.5$. For other MOSFET

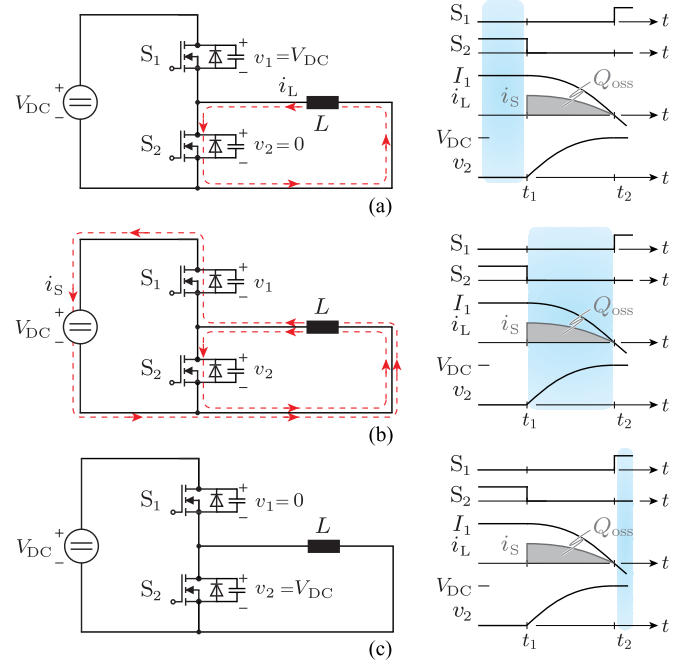


Fig. 3. Soft-switching transition of a MOSFET bridge leg and an inductor L : (a) free-wheeling interval with inductor current $i_L = I_1$; (b) switch S_2 turns off and resonant transition starts with additional current path through the dc source (For simplicity reasons, the parasitic output capacitances are assumed to be linear.); (c) end of transition when the drain–source voltage of S_2 has reached the source voltage, i.e., $v_2 = V_{DC}$, and switch S_1 turns on at zero voltage. As a result of the transition, the charge Q_{oss} was moved from switch S_1 to the dc source and the energy of the inductor L is zero whereas the total energy stored in the MOSFET bridge leg remains unchanged. Thus, the condition for complete soft switching equals $\frac{1}{2}LI_1^2 \geq Q_{oss}(V_{DC}) \cdot V_{DC}$.

devices, such as superjunction MOSFETs, the equivalent capacitances may even differ up to a factor of 4 to 5. This difference implies the necessity to clarify which equivalent capacitance has to be used in the case of modeling the soft-switching behavior of MOSFETs.

III. CONDITIONS FOR IDEAL SOFT-SWITCHING

In order to avoid the losses caused by hard-switching transitions of MOSFETs, ZVS is commonly applied. This requires the presence of an impressed current of an inductive component which charges/discharges the output capacitances of the MOSFETs within a bridge leg during the interlocking time of the associated gate signals, as visualized in Fig. 3 for a transition where switch S_2 turns off and S_1 turns on. The required energy of the inductance for a complete soft-switching transition can be found by considering the energy balance of

$$E_{initial} + E_{delivered} = E_{final} + E_{dissipated} \quad (3)$$

where $E_{initial}$ denotes the energy within the system for $t < t_1$ and E_{final} denotes the energy after the ZVS transition. $E_{delivered}$ is the energy which is delivered by the source and $E_{dissipated}$ is the energy which is dissipated during the ZVS transition which is assumed to be $E_{dissipated} = 0$. Furthermore, it is assumed that the switches S_1 and S_2 in the half-bridge are equal, which means that they exhibit the same nonlinear characteristic of C_{oss} in

dependence of V_{DS} . This is also typically the case in half-bridge configurations with bidirectional power flow capability.

At the beginning of the transition ($t < t_1$), the current i_L of the inductor is free-wheeling through S_2 and the output capacitance $C_{oss,1}$ of switch S_1 is charged to the source voltage V_{DC} . Assuming a linear inductance, the energy within the system for $t < t_1$ is, therefore, equal to

$$E_{\text{initial}} = E_{\text{oss}}(V_{DC}) + \frac{1}{2}LI_1^2. \quad (4)$$

During the switching transition ($t_1 < t < t_2$), the inductor and the capacitances of the switches form a resonant circuit. The current i_L is split up between both capacitances and charges $C_{oss,2}$ and discharges $C_{oss,1}$. In the case of a complete ZVS transition at the boundary to loosing ZVS, the charging/discharging process is finished at the same time (t_2) when the inductor current reaches $i_L = 0$ A which is also when switch S_1 is turned ON. Thus, the energy in the system after the ZVS transition equals

$$E_{\text{final}} = E_{\text{oss}}(V_{DC}) \quad (5)$$

and the energy received by the source during the transition equals

$$E_{\text{delivered}} = -Q_{\text{oss}}(V_{DC}) \cdot V_{DC} \quad (6)$$

since the charge of switch S_1 was moved by i_S to the source with voltage V_{DC} . As a result, the energy balance of (3) reveals that the requirement for a complete zero-voltage transition is given by

$$\frac{1}{2}LI_1^2 \geq Q_{\text{oss}}(V_{DC}) \cdot V_{DC}. \quad (7)$$

This requires the evaluation of the charge-equivalent (and *not* the energy-equivalent [6]–[9]) capacitance at the voltage V_{DC}

$$\frac{1}{2}LI_1^2 \geq C_{Q,\text{eq}}(V_{DC}) \cdot V_{DC}^2. \quad (8)$$

Please note that additional parasitic capacitances of the switch node (e.g., PCB capacitances and the parasitic capacitance of the inductor) also influence the required energy of the inductor for soft switching. The parasitic capacitances are assumed to be linear with respect to their capacitance value in dependence of the applied voltage, which allows us to lump them into a total parasitic capacitance C_{par} . Accordingly, considering Fig. 3 the energy term $\frac{1}{2}C_{\text{par}}V_{DC}^2$ has to be added to the right-hand sides of (7) and (8).

ZVS losses due to nonidealities: Even if the aforementioned condition for ZVS is fulfilled, switching losses might still be measured due to following two effects:

- 1) At large inductor currents, turn-off losses can occur if the gate drive circuitry is too slow to turn-off the semiconductor before the drain–source voltage rises. The resulting overlapping of drain–source current and drain–source voltage leads to losses within the semiconductor.
- 2) The charging/discharging process of the output capacitances is not free of losses [10]. For SiC MOSFETs, GaN HEMTs, and low-voltage Si MOSFETs, losses of up to 10% of the energy stored in the output capacitance could occur,

as indicated by measurements of the authors. For super-junction Si MOSFETs, however, the loss mechanism is a combination of a resistive and a diode-like component and might dissipate more than 50% of the stored energy. More details about the C_{oss} related losses can be found in [10] and [11]. As a result, a sufficiently larger energy has to be stored in L to achieve ZVS and/or even with ZVS significant switching losses can occur.

IV. INCOMPLETE SOFT-SWITCHING

Even if all nonidealities of real MOSFET circuits (cf., Section III) are disregarded, the soft-switching transition can result in losses if the condition for ZVS, (7), is not fulfilled and/or incomplete soft-switching [incomplete ZVS (iZVS)] occurs. This means that there is still a voltage ΔV present across the switch S_1 that turns on after the resonant transition. In order to calculate the remaining voltage ΔV , the energy expression E_{final} has to be revised to

$$E_{\text{final}} = E_{\text{oss}}(V_{DC} - \Delta V) + E_{\text{oss}}(\Delta V) \quad (9)$$

and the energy delivered by the source has to be changed to

$$E_{\text{delivered}} = -(Q_{\text{oss}}(V_{DC}) - Q_{\text{oss}}(\Delta V)) \cdot V_{DC}. \quad (10)$$

The value of ΔV can then be found by solving the energy balance of (3) (again for $E_{\text{dissipated}} = 0$). Please note that additional parasitic capacitances and resistive losses are not included in this equation.

In the iZVS transition, switch S_1 turns on while $C_{oss,1}$ is still charged to ΔV , which dissipates a certain amount of energy that can be derived by solving the energy balance of

$$E_{\text{diss, iZVS}} = E_{\text{initial, iZVS}} - E_{\text{final, iZVS}} + E_{\text{delivered, iZVS}}. \quad (11)$$

Before S_1 turns on, the energy within the system is equal to

$$E_{\text{initial, iZVS}} = E_{\text{oss}}(V_{DC} - \Delta V) + E_{\text{oss}}(\Delta V). \quad (12)$$

After S_1 has turned ON, $C_{oss,2}$ of switch S_2 is charged to V_{DC} , therefore

$$E_{\text{final, iZVS}} = E_{\text{oss}}(V_{DC}). \quad (13)$$

In order to charge the output capacitance of S_2 to V_{DC} , the remaining charge

$$\Delta Q_{S_2} = Q_{\text{oss}}(V_{DC}) - Q_{\text{oss}}(V_{DC} - \Delta V) \quad (14)$$

has to be taken from the source; accordingly the source delivers the energy

$$E_{\text{delivered, iZVS}} = \Delta Q_{S_2} \cdot V_{DC}. \quad (15)$$

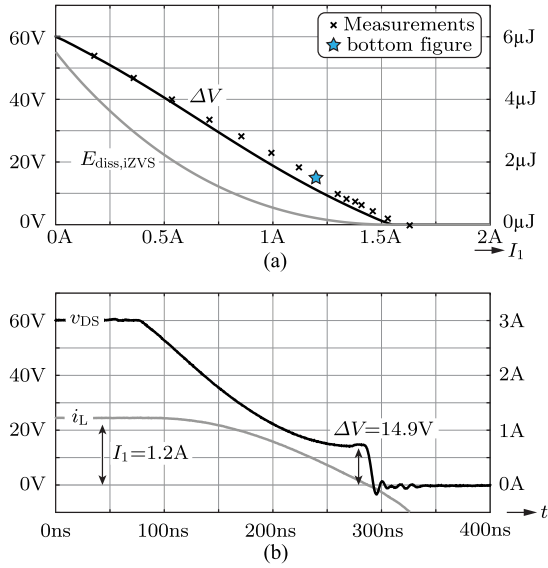


Fig. 4. Measurements of an iZVS transition with a MOSFET bridge leg (BS046N100NS3/Infineon) and an inductor with $L = 4.6 \mu\text{H}$: (a) calculated and measured remaining voltage ΔV [cf., (9)] across switch S_2 for different initial values of inductor current $i_L = I_1$ and the associated dissipated energy $E_{diss,iZVS}$ of an iZVS transition with remaining voltage ΔV ; (b) measured waveform of the drain–source voltage v_{DS} of switch S_2 and inductor current i_L for an initial inductor current value of $i_L = 1.2$ A.

As a result, the dissipated energy of the iZVS transition can be derived and interpreted as

$$\begin{aligned}
 E_{diss,iZVS} = & \underbrace{E_{oss}(\Delta V)}_{\text{① Energy dissipated in } S_1 \text{ when } S_1 \text{ turns on}} \\
 & + \underbrace{\Delta Q_{S_2} \cdot V_{DC}}_{\text{② Energy provided by source during turn-on of } S_1} \\
 & - \underbrace{(E_{oss}(V_{DC}) - E_{oss}(V_{DC} - \Delta V))}_{\text{Share of energy of ② which is stored in } S_2}. \quad (16)
 \end{aligned}$$

For the case of a complete soft-switching transition (i.e., $\Delta V \rightarrow 0$) the above equation yields $E_{diss,iZVS} \rightarrow 0$. For the second limit case of $\Delta V \rightarrow V_{DC}$, which denotes hard switching, the energy $E_{diss,iZVS} \rightarrow Q_{oss}(V_{DC}) \cdot V_{DC} = C_{Q,eq} \cdot V_{DC}^2$ can be used to estimate the losses which occur due to the parasitic output capacitance in the event of hard switching [5]. Please note again that in the case of incomplete soft-switching and also in the case of (full) hard switching, the charge-equivalent and *not* the energy-equivalent capacitance (as frequently used in literature) is relevant and, therefore, the actual switching losses are greater than switching losses estimated using the energy-equivalent capacitance. Furthermore, nonidealities resulting in additional losses are not included in the equations.

V. EXPERIMENTAL VALIDATION

The theoretical derivations of the previous sections have been experimentally validated and the results are shown in the following.

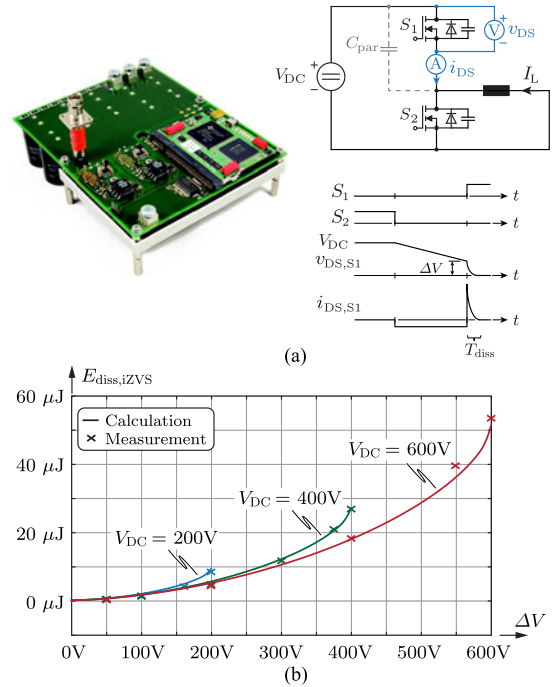


Fig. 5. Experimental verification of switching energies for iZVS with SiC MOSFETs: (a) measurement setup to determine the dissipated energy of S_1 which turns on with a nonzero drain–source voltage of $v_{DS,S1} = \Delta V$. The test bench employs a digital controller to generate the gate signals of the double pulse tests. High-bandwidth 1-GHz current shunts (SDN-414-10/T&M Research) are used to measure the currents by means of a coaxial cable whereas the voltages are measured with high-voltage passive probes. The schematic waveforms are split into the resonant transition phase (T_{res}) where energy is recovered from S_1 and a dissipative phase (T_{diss}) which occurs when switch S_1 is turned ON. The total dissipated energy $E_{diss,iZVS}$ for different dc-link voltages V_{DC} and different remaining voltages ΔV is shown in (b) as a comparison between measured and calculated values according to (16).

A. Incomplete Soft-Switching Transition

The incomplete soft-switching process was tested with a bridge leg containing two low-voltage MOSFETs (BS046N100NS3/Infineon) connected to a voltage source with $V_{DC} = 60$ V and an inductor with $L = 4.6 \mu\text{H}$. The voltage ΔV , which remains at the switch node after an incomplete soft-switching process, was calculated according to (4) and (9) and is shown in Fig. 4(a) for different values of the initial inductor current I_1 and compared to measurement results. The difference between the measurements and calculations can be attributed to ohmic losses in the conduction path (i.e., coil winding, MOSFETs, PCB) and to additional layout-dependent capacitances which require additional energy to be charged/discharged. In addition, the calculated value of the energy $E_{diss,iZVS}$ which is dissipated at this iZVS transition is also shown as a function of the initial inductor current. The transient waveforms of the inductor current and the bridge-leg voltage are depicted for an initial inductor current of $I_1 = 1.2$ A in Fig. 4(b).

B. Loss Measurements

In order to verify the derived formulas of Section IV of the switching losses occurring in case of incomplete

TABLE I
DETAILED COMPARISON OF SELECTED iZVS LOSS MEASUREMENT RESULTS
WITH CALCULATED VALUES

V_{DC}	ΔV	$E_{diss, iZVS, meas}$	$E_{diss, iZVS, calc}$	Error
200 V	200 V	8.26 μ J	8.39 μ J	1.5%
200 V	100 V	1.26 μ J	1.35 μ J	7.0%
200 V	50 V	0.273 μ J	0.318 μ J	13.9%
400 V	300 V	11.6 μ J	11.4 μ J	-1.8%
400 V	100 V	1.11 μ J	1.11 μ J	0.5%
600 V	400 V	18.1 μ J	18.1 μ J	0.4%
600 V	200 V	4.13 μ J	4.3 μ J	3.9%

soft-switching, a measurement setup for precise switching loss measurements [cf., Fig. 5(a)] was used with SiC MOSFETs (C2M0080120D/Cree) which have an almost ideal soft-switching behavior; accordingly the losses of the charging and discharging process of C_{oss} can be neglected (as discussed in Section III). In this setup, the current and voltage waveforms across the top switch S_1 are measured by means of a high-bandwidth oscilloscope and a current shunt which allows us to determine the energy released or stored by this switch during the incomplete soft-switching process and, thus, to verify (16). The experimental setup contains specific layout-dependent parasitic capacitances (e.g., probes, PCB) that are included in the calculation by means of a lumped capacitance, which was measured to amount to $C_{par} = 123$ pF. The energy stored in the parasitic capacitances is also dissipated in switch S_1 and has to be included in the calculations, which yields

$$E_{diss, iZVS, calc} = E_{diss, iZVS} + \frac{1}{2}C_{par}\Delta V^2. \quad (17)$$

The measurements were conducted for different levels of dc-link voltage V_{DC} and different levels of remaining midpoint voltage ΔV . The results are visualized in Fig. 5(b) and a detailed overview of the measurement results is provided in Table I. The theory is confirmed by the measurements with a high accuracy.

VI. CONCLUSION

In order to determine whether soft switching can be achieved in a circuit with a MOSFET bridge leg and an inductor carrying the initial current $i_L = I_1$, the stored charge Q_{oss} of the MOSFETs has to be considered and the condition

$$\frac{1}{2}LI_1^2 \geq Q_{oss}(V_{DC}) \cdot V_{DC} \quad (18)$$

has to be fulfilled. For the case that the condition for complete

soft switching is not fulfilled, the additional losses of the incomplete soft-switching process can be calculated based on the formulas derived in this letter. The formulas also allow to calculate the losses which occur due to the parasitic output capacitances in the event of (full) hard switching. The derived equations have been validated with high accuracy on dedicated measurement setups with low-voltage silicon MOSFETs and high-voltage SiC MOSFETs.

REFERENCES

- [1] J. W. Kolar, F. Krismer, Y. Lobsiger, J. Muehlethaler, T. Nussbaumer, and J. Minibock, "Extreme efficiency power electronics," in *Proc. 7th Int. Conf. Integr. Power Electron. Syst.*, 2012, pp. 1–22. [Online]. Available: <http://ieeexplore.ieee.org/stamp/stamp.jsp?tp=&arnumber=6185790>
- [2] S. Waffler and J. W. Kolar, "Comparative evaluation of soft-switching concepts for bi-directional buck+boost dc-dc converters," in *Proc. Int. Power Electron. Conf.*, 2010, pp. 1856–1865. [Online]. Available: <http://ieeexplore.ieee.org/stamp/stamp.jsp?arnumber=5542152>
- [3] C. Marxgut, J. Biela, and J. W. Kolar, "Interleaved triangular current mode (TCM) resonant transition, single phase PFC rectifier with high efficiency and high power density," in *Proc. Int. Power Electron. Conf.*, 2010, pp. 1725–1732. [Online]. Available: <http://ieeexplore.ieee.org/stamp/stamp.jsp?arnumber=5542048>
- [4] R. Miftakhutdinov, "New aspects on analyzing ZVS conditions for converters using super-junction Si and wide bandgap SiC and GaN power FETs," in *Proc. 16th Eur. Conf. Power Electron. Appl.*, 2014, pp. 1–9. [Online]. Available: <http://ieeexplore.ieee.org/stamp/stamp.jsp?arnumber=6911047>
- [5] F. Krismer, "Modeling and optimization of bidirectional dual active bridge dc-dc converter topologies," Ph.D. dissertation, *Power Electron. Syst. Lab.*, ETH Zürich, Zürich, 2010.
- [6] Texas Instruments, "Phase-shifted full-bridge, zero-voltage transition design considerations," *Tech. Rep. SLUA107A*, 2011.
- [7] T. Mishima and M. Nakaoka, "Practical evaluations of a ZVS-PWM dc-dc converter with secondary-side phase-shifting active rectifier," *IEEE Trans. Power Electron.*, vol. 26, no. 12, pp. 3896–3907, Dec. 2011.
- [8] B. Y. Chen and Y. S. Lai, "Switching control technique of phase-shift-controlled full-bridge converter to improve efficiency under light-load and standby conditions without additional auxiliary components," *IEEE Trans. Power Electron.*, vol. 25, no. 4, pp. 1001–1012, Apr. 2010.
- [9] J. W. Kim, D. Y. Kim, C. E. Kim, and G. W. Moon, "A simple switching control technique for improving light load efficiency in a phase-shifted full-bridge converter with a server power system," *IEEE Trans. Power Electron.*, vol. 29, no. 4, pp. 1562–1566, Apr. 2014.
- [10] J. Fedison, M. Fornage, M. Harrison, and D. Zimmanck, "C related energy loss in power MOSFETs used in zero-voltage-switched applications," in *Proc. 29th Annu. IEEE Appl. Power Electron. Conf. Expo.*, 2014, pp. 150–156. [Online]. Available: <http://ieeexplore.ieee.org/stamp/stamp.jsp?arnumber=6803302>
- [11] J. Fedison and M. Harrison, "COSS hysteresis in advanced superjunction MOSFETs," in *Proc. Appl. Power Electron. Conf. Expo.*, 2016, pp. 247–252.